Experimental study of radiation attenuation using water curtains in a reduced-scale deck a ro-ro ship

Davood Zeinali, Florian Inglod, Zoubir Acem, Rabah Mehaddi, Gilles Parent, Anthony Collin, Pascal Boulet

Experimental study of radiation attenuation using water curtains in a reduced-scale deck of a ro-ro ship

Davood Zeinali[1, 2], Florian Ingold[1], Zoubir Acem[1], Rabah Mehaddi[1], Gilles Parent[1], Anthony Collin[1], Pascal Boulet[1]

[1] *Université de Lorraine, CNRS, LEMTA, F-54000 Nancy, France*

[2] *Corresponding author*: davood.zeinali@univ-lorraine.fr

ABSTRACT

Experiments have been conducted at LEMTA to evaluate the containment of thermal radiation using water curtains in a model setup of a ro-ro ship's cargo deck with a scale of 1 to 12.5, providing data for future numerical simulations. The water curtains are created with one or two rows of water mist nozzles at pressures ranging from 3 to 8 bar, while the radiation source is an electric black body at 550ºC. The containment effect in terms of radiative attenuation is evaluated by comparing the radiation levels with and without water curtains measured using a multispectral infrared camera.

Keywords: *water curtain, radiation, ro-ro ship, cargo deck*

1. INTRODUCTION

Roll-on/roll-off vessels, commonly referred to as ro-ro ships, are large ships used to transport wheeled cargo such as trucks and trailers, loaded onto the ship using built-in ramps. Ro-ro ships can also be passenger ships, customarily known as ferries. To reduce the danger and cost of fires aboard such ships, it is necessary to study the capabilities for containment of heat and smoke in their long cargo decks. Correspondingly, experiments have been conducted at LEMTA to evaluate the containment of thermal radiation using water curtains in a model setup of a ro-ro ship's cargo deck, as part of the international research project of LASHFIRE (Legislative Assessment for Safety Hazards of Fire and Innovations in Ro-ro ship Environment), which is funded by the European Union and involves 27 research and industry partners from 13 European Union member states.

The general objective of the LASHFIRE project is to enhance the safety of ro-ro ships, providing the maritime industry with new knowledge to build safer and more competitive ships for sustainable transport. The role of LEMTA in this project is to study the possibility of smoke and heat containment by means of vertical divisions created using fabric or water curtains.

Fire containment by water curtains has been widely explored in the literature in various contexts (Blanchard et al., 2014, Parent et al., 2016a, Mehaddi et al., 2020, Parent et al., 2006, and Collin et al., 2007). However, radiation containment by water curtains in the maritime context is understudied. This is the motivation behind the present experimental study which considers the impact of the ship's cargo deck geometry on the water curtain and its capability for containment of radiation.

Stopping radiation from reaching other parts of the ship plays an important role in preventing fire propagation. In this study, the position and

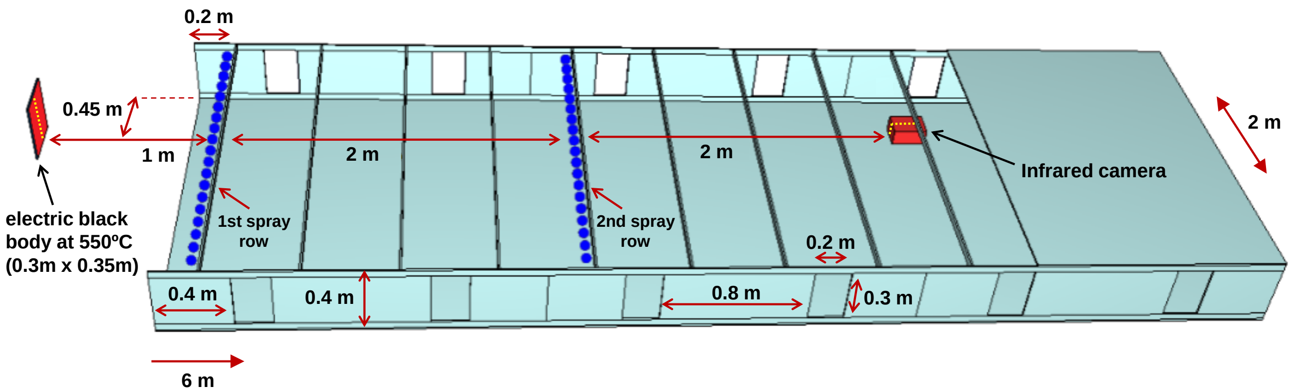

Figure 1 A sketch of the model cargo deck setup made of transparent polycarbonate, showing the position of the black body and the infrared camera with respect to the two rows of water spray systems (each consisting of 19 mist nozzles). The ceiling is shown partially to visualize the interior.

number of rows of water mist curtains and their flowrate are varied to evaluate their effects on the radiation containment capability.

The experiments are conducted in a reduced-scale setup as a practical means of investigating the role of factors such as flowrate and size of the injected water droplets on the radiative shielding mechanisms of the spray curtains.

The setup consists of a model cargo deck with a scale of approximately 1 to 12.5, incorporating water curtains made up of water mist nozzles. Moreover, an electric black body at a constant temperature of 550°C is used as the radiation source.

To quantify the level of radiation containment by the water curtains, an infrared camera is used. Correspondingly, the radiation levels measured without and with water curtain(s) are compared to calculate the containment efficiency in terms of radiative transmission and attenuation values, as explained by Buchlin (2005) and Parent et al. (2016b). Moreover, the experiments have been repeated several times to verify the repeatability of the observations.

The influence of wavelength on radiation attenuation, reported by Tseng & Viskanta, (2007) and Widmann & Duchez (2004), is evaluated in the present study using several filters mounted on the infrared camera, providing insight on the radiation attenuation capability of water mist curtains at different wavelengths.

2. METHODS

2.1 Model cargo deck

A schematic of the model cargo deck setup is shown in Fig. 1. The model has a scale of 1 to 12.5 with respect to the dimensions of a typical ro-ro ferry, namely Stena Flavia. The free height of the ship's cargo deck is approximately 5 m, corresponding to a height of 0.4 m in the model setup. The length of the cargo decks ranges from 100 m to 155 m, while the width ranges from 18 to 24 m. Correspondingly, the length and width of the model setup are 8 m and 2 m, respectively.

The model cargo deck setup is split into 4 detachable sections, each measuring 2 m in length. These can be moved to rearrange the deck sections as desired for different tests. In the radiation tests, the black body is situated at the center of the first section, but this section itself is not used due to the size of the black body.

2.2 Water spray system

As shown in Fig. 1, the spray system consists of two rows of water curtains, each with 19 water mist nozzles (type TP400067 from

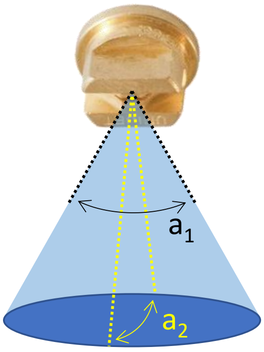

Figure 2 The spray pattern of a water mist nozzle characterized using one large angle (a_1) and one small angle (a_2).

Spraying Systems Co., with an orifice diameter of 530 µm). Between each two successive nozzles there is a distance of 0.1 m, and the nozzles are at 0.38 m height with respect to the floor of the deck in the setup, i.e., the distance of the injection point of the nozzles to the deck's ceiling is 0.02 m.

The spray pattern of each water mist nozzle resembles an elliptical cone which can be characterized using one large angle and one small angle as shown in Fig. 2. These spray angles have been presented in Table 1 for the water pressures tested in the present study. The nozzles in the model cargo deck setup are fixed such that the large spray angle aligns with the width of the deck (measuring 2 m as shown in Fig. 1) while the small spray angle is aligned with the length of the deck.

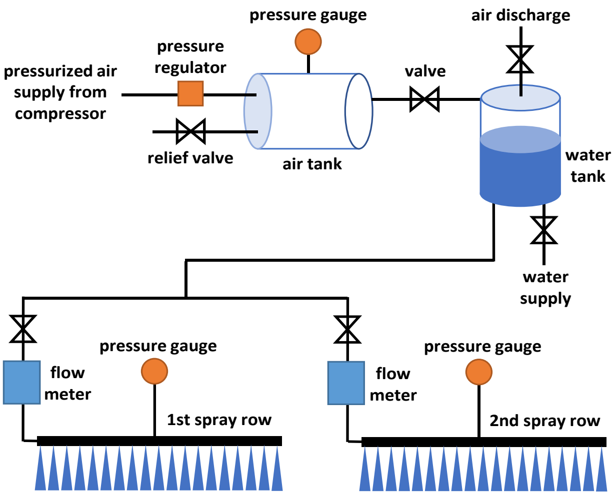

Figure 3 Setup of feed water system for the two rows of water spray curtains shown in Fig. 1.

A schematic of the feed water system is shown in Fig. 3. The system consists of a compressor capable of providing air with a maximum pressure of 10 bar. Using a pressure regulator, the air is stored at the desired pressure in an air tank. This regulated supply of air is then used to pressurize the feedwater in the water tank, capable of holding up to 30 liters of water. Correspondingly, the feedwater tank provides pressurized water to the two rows of water mist nozzles, with a pressure gauge at the center of each row recording the pressure with an accuracy of 10 millibars. Moreover, two flowmeters are used to monitor the total flowrate of each spray row with an accuracy of 0.1 L/min, and several valves are used to allow the regulation of pressure and water supply as desired. This feed water setup is similar to the one used by Parent et al. (2006).

Table 1 The flow rate and spray angles of the water mist nozzles in the present study

Pressure [bar]	3	5	8
Flow rate [L/min]	0.2	0.3	0.4
Large angle of spray* [°]	40	50	55
Small angle of spray* [°]	17	19	21

* Angles shown in Fig. 2.

Table 2 The scale of the model setup's geometry and water mist curtains with respect to those of a ro-ro ship

Feature	**Model**	**Ship**	**Scaling factor**
Deck height [m]	0.4	5	$\alpha = 12.5$
Deck length [m]	8	100	α
Deck width [m]	2	25	α
Water flow rate per nozzle [L/min]	0.2-0.4	110-220*	$\alpha^{5/2}$ **
Mean diameter of droplets [µm]	130-170***	460-600	$\alpha^{1/2}$ **
Mean velocity of droplets [m/s]	14-22***	50-78	$\alpha^{1/2}$ **

* The total capacity of the water pumps on the ships can typically range from 1800 to 16000 L/min.

** Based on scaling correlations reported by Yu (2012).

*** See Figs. 4 and 5.

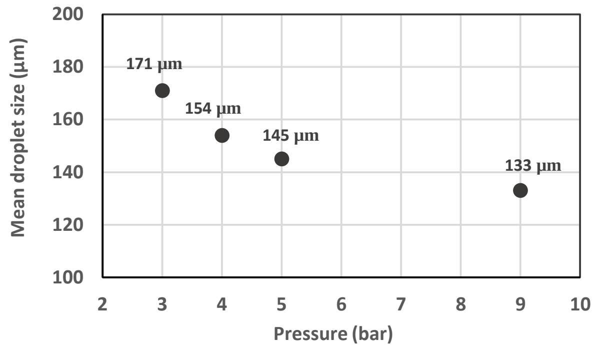

Figure 4 Mean droplet diameter (D_{50} in µm) measured at 0.2 m distance below the injection point of the water mist nozzle (type TP400067 from Spraying Systems Co.)

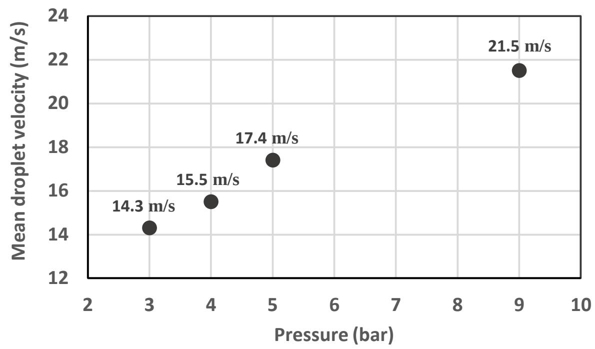

Figure 5 Mean droplet velocity (V_{50} in m/s) measured at 0.2 m distance below the injection point of the water mist nozzle (type TP400067 from Spraying Systems Co.)

Even though the geometrical size of the model yields a scaling factor of 12.5, a different scaling factor is needed for the design of the flow rate and droplet diameter of the water curtains in the reduced-scale model. A prominent literature reference used for general scaling purposes in fire research is the work of Quintiere (1989) and a useful summary of the related heat transfer relations has been provided by Drysdale (2011). For the specific application of fire suppression systems, more scaling relations have been reported by Yu (2012), with the related characteristics of water mist systems detailed in the SFPE Handbook of Fire Protection Engineering (Mawhinney and Back, 2016). Table 2 shows the scaling of the model setup's different features with respect to those of a ro-ro ship based on the aforementioned principles.

Figure 6 A photo of the electric black body used in the experiments. The control box underneath makes it possible to adjust the surface temperature and the internal ventilation of the black body equipment.

To evaluate the impact of the number of water curtains and their position on the level of radiation containment, the two rows of water curtains are placed at different distances from the radiation source and are used one at a time or both at the same time. Moreover, to examine the influence of water flow rate, experiments are conducted at flow rates ranging from 0.2 to 0.4 L/min/nozzle. The nomenclature of the conducted experiments is presented in Table 3.

2.3 Black body

To produce a constant level of incident radiation for attenuation measurements in all the experiments, an electric black body is used (model ECN100 from HGH Infrared Systems), operating with a single-phase alternating current at 230 volts and 50 Hz. The radiating surface of the black body is 0.3 m wide and 0.35 m high, with a fixed temperature of 550°C, with its center being at the mid height of the model deck setup. Figure 6 shows a photo of the black body.

Table 3 Nomenclature of the experiments

	Flow rate per nozzle (L/min)	**Row of water curtain used****
Test 1	0.2	1st
Test 2	0.2	2nd
Test 3	0.2	Both
Test 4-1*	0.3	1st
Test 4-2*	0.3	1st
Test 5	0.3	2nd
Test 6	0.3	Both
Test 7-1*	0.4	1st
Test 7-2*	0.4	1st
Test 8	0.4	2nd
Test 9	0.4	Both

* Repeated test

** The two rows of water curtains are shown in Fig. 1.

2.4 Infrared camera

The infrared camera (model MS M1K from TELOPS) incorporates 7 filters, capable of targeting the peak emission wavelengths of combustion products such as water vapor (H_2O), carbon dioxide (CO_2) and soot, i.e., species responsible for the bulk of thermal radiation from a fire (Drysdale, 2011). Table 4 lists the wavelength range of the aforementioned filters.

Table 4 Wavelength range of the infrared camera's filters

	Wavelength range [μm]
Filter 1	[1.500 5.000]
Filter 2	[2.291 2.333]
Filter 3	[3.376 3.444]
Filter 4	[3.762 3.838]
Filter 5	[3.983 4.035]
Filter 6	[2.832 2.889]
Filter 7	[4.400 4.457]

For each experiment, the infrared camera first observes the black body alone for approximately 20 s, then the water mist curtains are activated for a period of 20 s, after which they are deactivated and the infrared camera continues to observe the black body for 20 s.

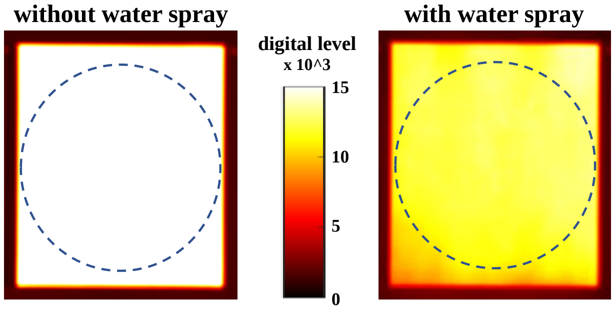

Figure 7 Time-averaged infrared images of the black body in test 6 based on the digital data of the camera (filter 1). The data is averaged over a period of 10 s before the water curtain activation (left) and after the water curtain activation (right). The area in the dashed circle is used for spatial averaging (see Fig 8).

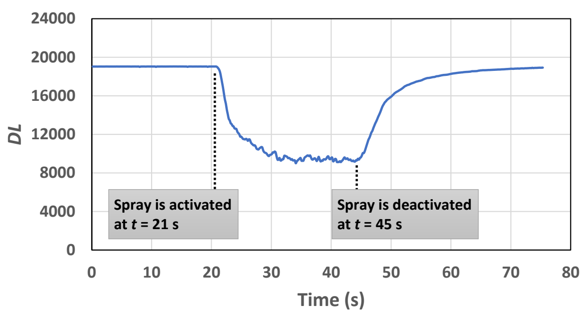

Figure 8 The temporal evolution of the digital levels recorded by the infrared camera (filter 1) averaged over the surface of the back body in test 6. The values before and after the activation of the water spray correspond to $DL_{\text{without spray}}$ and $DL_{\text{with spray}}$ in Eq. (1), respectively.

Accordingly, time-averaged images of the black body can be obtained based on the digital data, as shown in Fig. 7.

The radiative attenuation is quantified based on the digital levels measured by the infrared camera without and with water spray curtain(s) as follows (Zhu et al., 2015, Parent et al. 2016b):

$$A = \left(1 - \frac{DL_{\text{with spray}} - DL_0}{DL_{\text{without spray}} - DL_0}\right) \times 100 \qquad (1)$$

A is the percentage of radiative attenuation and DL stands for the digital levels recorded by

Table 5 Radiative attenuation levels (%) for all the conducted tests and different camera filters

	Mean	**Filter 1**	**Filter 2**	**Filter 3**	**Filter 4**	**Filter 5**	**Filter 6**	**Filter 7**
Test 1	11	11	10	11	11	12	13	12
Test 2	21	21	19	21	21	22	23	22
Test 3	48	49	44	48	48	49	47	50
Test 4-1	32	32	28	32	31	33	32	33
Test 4-2	36	37	32	36	36	37	36	38
Test 5	36	36	33	36	36	37	36	37
Test 6	54	54	49	54	54	55	53	56
Test 7-1	64	65	59	65	65	65	63	67
Test 7-2	64	65	59	65	65	65	64	66
Test 8	66	67	62	67	67	68	65	69
Test 9	80	81	75	80	80	81	78	82

the infrared camera, which are to be averaged over the surface of the black body over a period of 10 s. Correspondingly, $DL_{\text{with spray}}$ and $DL_{\text{without spray}}$ denote the average DL values for the duration of water spray activity and the duration of no water spray activity, respectively (see Fig. 8). Moreover, DL_0 denotes the average DL value when the lens of the camera is covered with a lid to calibrate the 'zero' level of radiation.

3. RESULTS AND DISCUSSION

The attenuation results for all the conducted experiments are presented in Fig. 9 and tabulated in Table 5. Moreover, the mean attenuation values have been visualized in the form of a 3D envelope in Fig. 10.

A higher level of radiative shielding is observed at higher water flowrates mainly due to the higher number of water droplets and the higher volume fraction of water, causing 45 to 53% more radiative attenuation when the flowrate is doubled (see Fig. 10).

Another reason for the increased radiative shielding at higher water flowrates is the reduced size of the droplets at higher water pressures (see Fig. 4), increasing the scattering and absorption efficiency of the spray (Oluwole et al., 2021).

The level of radiative shielding provided by a single water curtain is almost unaffected by the

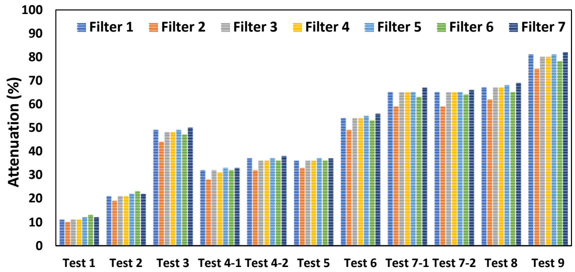

Figure 9 Radiative attenuation levels obtained for all the conducted experiments. The filtered wavelength ranges are those in Table 4.

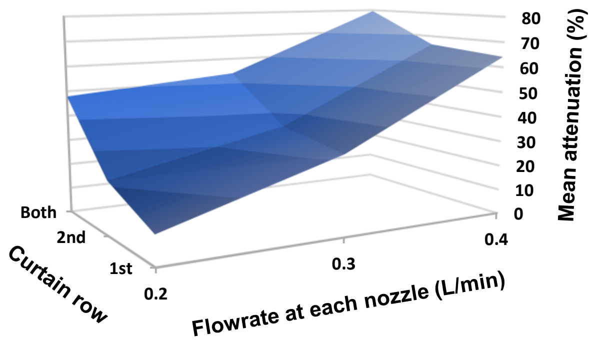

Figure 10 The envelope of mean radiative attenuation levels obtained for different flowrates and numbers of water curtains. See Fig. 1 for the location of '1st' and '2nd' curtains.

location of the curtain for cases with water pressures between 5 and 8 bar, with all the attenuation levels being within ±3% of each other. This falls within the range of variations in the repeatability experiments, i.e., ±5%. This is while at a water pressure of 3 bar, the curtain located further away from the radiation source yields attenuation levels which are nearly 100%

higher than those of a curtain close to the radiation source (compare tests 1 and 2 in Table 5). This is expected to be mainly due to smaller spray angles at the water pressure of 3 bar (see Table 1), influencing the radiation view factor of the water curtain with respect to the radiation source and the infrared camera.

Configurations with two water curtains provide higher levels of radiative attenuation compared to those with one curtain (by 14 to 37%). Correspondingly, the highest attenuation level is obtained with two rows of water curtains and a pressure of 8 bar, i.e., test 9 yielding an attenuation of 80%, although attenuation levels closer to 100% are still possible at higher water pressures (Zhu et al., 2015).

The attenuation level is more strongly influenced by the water flowrate than by the number of curtains, as suggested by the steeper slope of the 3D envelope in Fig. 10 along the flowrate axis. In other words, a configuration with a high flowrate supplied to one curtain provides a higher radiative shielding than a configuration with two curtains and an identical total flowrate. This lower radiative shielding observed in the latter configuration with two curtains is due to the lower flowrate at each individual curtain, creating a narrower spray pattern (see Table 1) and bigger water droplets. This is less efficient for shielding against radiation compared to the wider spray pattern and finer droplets produced by a single curtain at a high flowrate. Correspondingly, the test with one curtain and a flowrate of 0.4 L/min/nozzle shows a radiative attenuation level which is 18% higher than that of the test with two curtains and a flowrate of 0.2 L/min/nozzle, but also 10% higher than that of the test with two curtains and a flowrate of 0.3 L/min/nozzle.

In terms of wavelength dependency, the radiative shielding capability of the curtains shows only 3 to 8% variation in the range of 1.5 to 5 µm captured by the different filters of the infrared camera (see Fig. 9). This is because of the size of the water droplets being higher than 130 µm (Fig. 4). More considerable attenuation variations are expected across the wavelength spectrum for water droplets with diameters well below 100 µm (Widmann and Duchez, 2004).

4. CONCLUSIONS

In order to evaluate the containment of radiation using water curtains in a ro-ro ship's cargo deck and to provide data for future numerical simulations, a series of experiments have been conducted at LEMTA as part of the international project of LASHFIRE, using a model cargo deck with a scale of 1 to 12.5. An electric black body at a constant temperature of 550°C is used as the radiation source while the water curtains are created at pressures ranging from 3 to 8 bar using water mist nozzles.

Firstly, the position of the curtain does not seem to have a significant impact on the attenuation level at water pressures at or above 5 bar. Secondly, the water curtain yields higher attenuation levels at higher water flowrates and water pressures (by up to 53%). Moreover, the attenuation level increases with the number of water curtains (by up to 36%). In this regard, water flowrate and pressure seem to be more influential than the number of water curtains for radiative attenuation. That is to say, one curtain with a high flowrate provides a higher radiative shielding compared to two curtains with an identical total flowrate, with an attenuation difference of up to 18%. Lastly, the experiments suggest that the water mist curtains with droplets bigger than 130 µm offer a radiative shielding capability not strongly dependent on the wavelength (in the range of 1.5 to 5 µm).

5. ACKNOWLEDGMENTS

This work was funded by European Union's Horizon 2020 research and innovation program through grant agreement no. 814975 as part of the international research project of LASHFIRE.

Funded by the
European Union

6. REFERENCES

Blanchard, E., Boulet, P., Fromy, P., Desanghere, S., Carlotti, P., Vantelon, J.P., Garo, J.P., 2014, "Experimental and numerical study of the interaction between water mist and fire in an intermediate test tunnel," Fire Technology, Vol. 50, pp. 565-587.

Buchlin, J.-M., 2005, "Thermal shielding by water spray curtain," Journal of Loss Prevention in the Process Industries, Vol. 18, pp. 423-432.

Collin, A., Boulet, P., Parent, G., Lacroix, D., 2007, "Numerical simulation of a water spray—radiation attenuation related to spray dynamics," International Journal of Thermal Sciences, Vol. 46, pp. 856-868.

Drysdale, D., 2011, "Heat Transfer, An Introduction to Fire Dynamics," 3rd Edition, pp. 35-82.

Lechêne, S., Acem, Z., Parent, G., Collin, A., Boulet, P., 2012, "Radiative shielding by water mist: comparisons between downward, upward and impacting injection of droplets," Journal of Physics: Conference Series, Vol. 369, pp. 012-027.

Mehaddi, R., Collin, A., Boulet, P., Acem, Z., Telassamou, J., Becker, S., Demeurie, F., Morel, J.-Y., 2020, "Use of a water mist for smoke confinement and radiation shielding in case of fire during tunnel construction," International Journal of Thermal Sciences, Vol. 148, pp. 106-156.

Mawhinney, J.R., and Back III, G.G., 2016, "Water mist fire suppression systems," SFPE Handbook of Fire Protection Engineering 5th Edition, pp. 1587-1645.

Oluwole, O.O., Gupta, A., Wu, B., Zhao, X., Meredith, K.V., Wang, Y., 2021, "Nongray models for radiative absorption and anisotropic scattering by water droplets in fire CFD simulations," Fire Safety Journal, Vol. 120, 103034.

Parent, G., Morlon, R., Acem, Z., Fromy, P., Blanchard, E., Boulet, P., 2016a, "Radiative shielding effect due to different water sprays used in a real scale application," International Journal of Thermal Sciences, Vol. 105, pp. 174-181.

Parent, G., Morlon, R., Acem, Z., Fromy, P., Blanchard, E., Boulet, P., 2016b, "Radiative shielding effect due to different water sprays used in a real scale application," International Journal of Thermal Sciences, Vol. 105, pp. 174-181.

Parent, G., Boulet, P., Gauthier, S., Blaise, J., Collin, A., 2006, "Experimental investigation of radiation transmission through a water spray," Journal of Quantitative Spectroscopy and Radiative Transfer, Vol. 97 (1), pp.126-141.

Quintiere, J.G., 1989, "Scaling applications in fire research," Fire safety journal, Vol. 15, pp. 3-29.

Tseng, C.C, .Viskanta, R., 2007, "Absorptance and transmittance of water spray/mist curtains," Fire Safety Journal, Vol. 42, pp. 106-114.

Widmann, J.F., Duchez, J., 2004, "The effect of water sprays on fire fighter thermal imagers," Fire Safety Journal, Vol. 39, pp. 217-238.

Yu, H.Z., 2012, "Froude-modeling-based general scaling relationships for fire suppression by water sprays, Fire Safety Journal, Vol. 47, pp. 1-7.

Zhu, P., Wang, X., Wang, Z., Cong H., and Ni, X., 2015, "Experimental and numerical study on attenuation of thermal radiation from large-scale pool fires by water mist curtain," Journal of Fire Sciences, Vol. 33(4), pp. 269-289.